Modelling and Simulation by Bond Graph Technique of a DC Motor FED from a Photovoltaic Source Via MPPT Boost Converter

R.Andoulsi (1), A.Mami (2), G.D. Tanguy (3), M.Annabi (4)

(1) Institut National de Recherche Scientifique et Technique B.P. 95 Hammam-Lif 2050 Tunisie.
Fax: 216(1)430.934 _ Tel:216(1)430.044
(2) Faculté de sciences de Tunis C.U Belvédère 1060 Tunis. Tunisie. Fax: 216(1)885.073
(3) LAIL, URA CNRS D1440, Ecole Centrale de Lille. B.P.48, 59651 Villeneuve d'ascq. Cedex France.) Fax: (33)320 335418
(4) Ecole Supérieure de Sciences Techniques. 5 AV Taha Houssein 1008 Tunis. Tunisie

Abstract : Optimum matching of loads to Photovoltaic (PV) generator is most desirable for more accurate sizing. Because of the relatively high cost of the PV generator, the system designer is mainly interested in its full utilisation by optimum matching of the system components during the entire operating period.

To achieve an optimum matching of the output characteristics of the PV source to the input characteristics of electromechanical loads, controlled converters are used. The converters topologies are function of optimal PV array and load parameters.

Application of PV power to electromechanical loads requires an understanding of the dynamics of such systems. As a very convenient and powerful tool for dynamic modelling, bond graph technique was used. The application of bond graph technique for the modelling of PV systems is not yet widespread.

The purpose of this work is to study the dynamic behaviour of a class of PV systems composed of a PV generator, a DC motor, and a boost DC-DC converter. The graphical approach based on bond graph methodology is used to formulate the dynamic model of this PV system. To develop that model, we take into account the non-linear device volt-ampere characteristic PV generator and we use averaged model DC-DC converter. Causality problems are discussed and a simplified model is deduced in order to give information from control loop point of view.

Time responses are simulated and stability domain is computed. A performance comparison between buck and boost converters showed disadvantages of these latter topologies in such application. In fact, results showed the existence of non minimal phase responses caused by positive real roots in the transfer function velocity numerator. This situation leads to mechanical problems hardly bearable by electromechanical machines. IMACS/IEEE CSCC'99 Proceedings, Pages:2591-2599

Keys- Words: Bond graph, photovoltaic, modelling, simulation, boost converter, MPPT,

Acronyms: photovoltaic:PV, direct current: DC

1 Introduction

The photovoltaic system technologies have increasing roles in electric power technologies, providing more secure power sources and pollution-free electric supplies. However in PV systems, the PV arrays costs are still relatively high and the energy conversion efficiency is quite low. Therefore the electric power generated by the PV arrays should be efficiently utilised.

In a direct coupled (with no battery storage) PV system, the solar cell array is directly connected to the motor load couple. These systems are relatively simple and inexpensive to operate. A direct coupled system may include a maximum power point tracker (MPPT) to improve its performance at starting and at steady state operation whenever it is needed [12].

The system under study consists of three different components; the PV generator, the DC-DC converters and the DC motor. Each component has its own operating characteristics which is the volt ampere characteristics for the PV generator and DC motor, torque speed for the mechanical load and the switch duty-cycle for the DC-DC converters.

The DC motor is supplied from the PV generator whose volt-ampere characteristics depend non-linearly on the solar insulation and temperatures variations and on the current drawn by the DC motor. To match the point at which the PV generator power is maximum, two solutions are generally available to the system designer. A) Carefully select the DC motor and the pump so that they match as closely as possible the maximum power line of the PV generator, or B) Use an electronic device (converters) known as MPPT, which continuously matches the output characteristics of the PV generator to the input characteristics of the DC motor [1].

The system under study in this paper is an application of the second option.

Before reaching the problem of controlled DC-DC converters we require understanding of the dynamics of such PV systems.

Investigations [4],[7], into the dynamic behaviour of PV systems have been conducted. Classical modelling and simulation have been done to predict the dynamic response of several photovoltaic system designs.

Due to its ease in handling dynamic systems and as a power tool for modelling we used the bond graph technique to study the dynamic behaviour of our PV systems.

The PV generator is characterised by a strongly non-linear current-voltage characteristics. A nonlinear state equation deduced from bond graph is given and a linearised model was then performed around the peak power point of the I-V characteristic.

From the state equation we deduce the transfer function and we study the PV system stability. We compute non minimal phase responses for a limited voltage PV generator area.

2 Bond graph model of the PV system

The bond graph approach has been developed in recent years as a powerful tool for modelling dynamic systems. It essentially focuses on the exchange of energy between the system and its environment and between different elements within the system. It is this energy exchange that determines the dynamics of any system [10].

To make the bond graph model we focus on the energetical structure of the PV system involved. Thereafter, a causality analysis is done in order to obtain a mathematical representation that fits into our need which is the study of dynamic behaviour from control loop point of view.

In order to develop a suitable bond graph of the PV system shown in figure 3, it’s necessary to understand the operating mode and the dynamics of each component

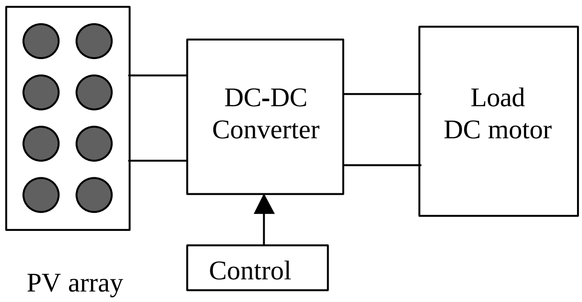

Fig.1. PV system configuration

2.1. PV generator

A PV generator consists of an array of photovoltaic cell modules connected in series parallel combination to provide the desired DC voltage and current.

Simulation of PV array operation can be described using a complete physical-mathematical model as shown in figure 2.

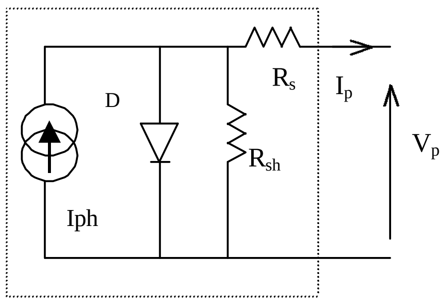

Fig. 2. Complete physical-mathematical PV array model

The current_voltage characteristic, strongly non-linear, can be represented by the following equation:

$$I_p = I_{ph} - I_s(\exp[\frac{q(V_p + I_p R_s)}{AKT}] - 1) - \frac{V_p + I_p R_s}{R_{sh}} \quad (1)$$

where I_p is the current, I_{ph} is the photo current, I_s is the reverse saturation current, q is the electron charge, V_p is the terminal voltage , R_s is the serial resistance , A is the idealité factor , k is the Boltzman constant, T is the absolute temperature and R_{sh} is the shunt resistance.

Under stable atmospheric conditions, the modelled PV generator I_V and P_V characteristics are given by figure 3. These ones are function of solar radiation

P_L, and panel temperature T. An identification algorithm was used to determine the PV array model parameters: $R_s, R_{sh}, I_s, I_{ph} \cdots$

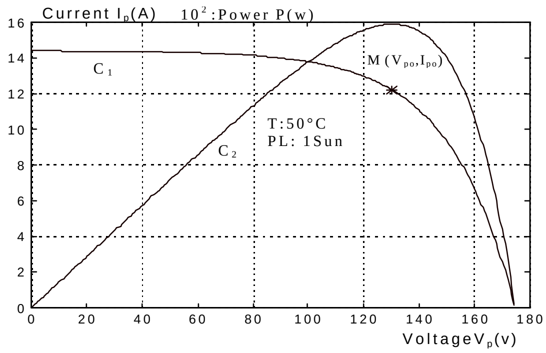

Fig.3. PV generator current -voltage (C_1) and power_voltage (C_2) characteristics

For the PV generator two resistances are often defined:

$$R_{st} = V_p / I_p \;.. \quad (2)$$

$$R_d = -(dV_p / dI_p) \;.. \quad .... (3)$$

where R_{st} represents the instantaneous PV array resistance and R_d the PV array dynamic resistance.

If R_{st} and R_d are known, it is possible to establish whether the array voltage is greater or less than the peak power voltage.

The condition of a maximum power point is given by:

$$\frac{d}{dV_p}[V_p \quad I_p] = 0 \quad (4)$$

The corresponding voltage V_{po} and current I_{po} are determined by solving equation (4) with an iterative method. At V_{po}, R_{st} is equal to R_d.

The bond graph representation of the PV array is given in figure 6. This device is modelled by a flow source $S_f = I_{ph}$ in parallel with the R elements which represent respectively the PV diode with its non-linear current voltage characteristic noted R_D and shunt resistance R_{sh}. With the later elements, we add the PV array serial resistance R_s.

2.2 MPPT converter

To attempt the optimal point, the DC motor is matched to the solar array by means of maximum power point tracker (MPPT). The MPPT consists of a power processing circuit, as buck or boost converters (Fig. 4), controlled by a signal source unit. In classical modelling this power processing circuit of the MPPT is often modelled by a controlled time variable transformer in which the transformation ratio m is changed continuously, corresponding to a variation in the load operating point [12]. The input/output equations of the time variable transformer are: $\begin{bmatrix} V_1 \\ I_1 \end{bmatrix} = \begin{bmatrix} m & 0 \\ 0 & m^{-1} \end{bmatrix} \begin{bmatrix} V_2 \\ I_2 \end{bmatrix}$

(5)

where m is the transformation ratio .

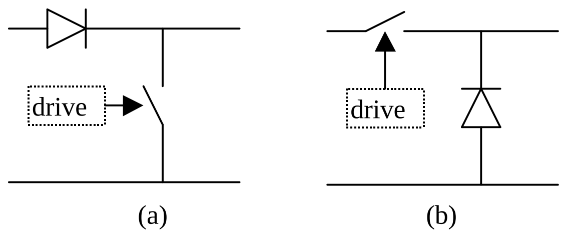

Fig. 4. Ideal switch model of boost (a) and buck (b) converters

For theses MPPT electronic devices (buck and boost converters), we used averaged bond graph models based on causality analysis proposed by B.Allard et al in [2]. The buck and boost converters are modelled by modulated transformers $MTF(\frac{1}{\rho})$ and $MTF(1-\rho)$ respectively. ρ is the controlled -switch duty cycle. We used this averaged bond graph model because it gives information about the behaviour from control loop point of view. In fact, since our great interest is to match the maximum power point when both solar insulation level and temperature change. This graphical representation will be helpful and easily used for the design and optimisation of the converter controls.

2.3 DC motor

The motor is a permanent-magnet DC motor represented by e.m.f Em, the armature circuit resistance R_m and inductance L_m , the inertia J, and the friction coefficient F. The DC motor is assumed to drive a centrifugal pump characterised with a torque proportional to angular velocity [4][7]:

$$\Gamma = K_T \Omega \text{ and } E_m = K_b \Omega . \tag{6}$$

Γ is the applied shaft torque, Ω the shaft angular velocity, K_T , K_b are the proportionality factor between shaft torque, back emf and angular velocity respectively.

This permanent-magnetic DC motor is represented by a classical bond graph model in which the flows at the junctions (1 - 20 21 22 53) and (1- 31 32,33,34) represent the armature current and the mechanical rotation speed respectively. The mechanical load, characterised by proportional torque to angular velocity (centrifugal pump), is represented by an R element R:KT.

2.4 Storage Capacitor

High power is temporarily required to overcome the break away torque and to start up the system. This power can not be delivered by the PV array and has to be provided by a storage device (electrolytic capacitor) C_p. Further more a minimum speed is necessary to guarantee the lubrication of rotor and stator start.

The equivalent electrical circuit and the bond graph model corresponding to the PV system under study are shown in Fig.5 and Fig.6 respectively.

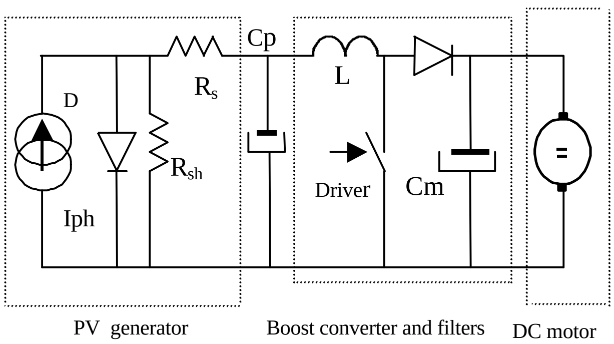

Fig.5. Equivalent electrical circuit of the PV system

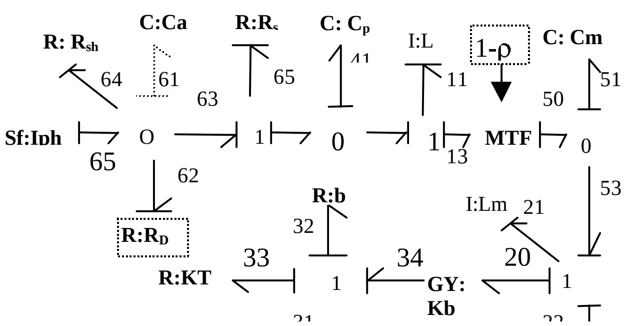

From this model, it can be seen that the resistance R_{sh}, and R_D introduce uncertainty in the causal structure. If the conductance causality is assigned to R_{sh}, then R_D will have a resistance one. This introduces an algebraic loop between R_{sh} and R_D as the flow in R_{sh} depends upon the effort given by R_D, which in turn, is a function of the flow given by R_{sh} [9][10].

In order to solve the problem of causal uncertainty, we propose to add an element C:(C_a) on the bond graph at the first 0-junction, that is in parallel on the current source. This element has to be of small value and will be suppressed in the mathematical model by applying the singular perturbation method while considering the state variable associated with the added element as very fast[6]. The validity of this approach can be physically interpreted. In fact the capacitor C_a exists in a solar cell but its effect is negligible unless the frequency of the system is very high. Cp is the diode capacitance due to the depletion region and the diffusion of carriers. It has a very low capacitance of the magnitude order of 10^{-9} μF and is a function of irradiance, cell temperature cell operating voltage , current, etc.. Unfortunately, during simulation it was observed that solution becomes very stiff and simulation with this representation becomes impractical [10].

Since our objective is to study, in a first analysis, the stability of this controlled PV system, we overcome the difficulty cited above by using the simple PV array model commonly used in which the effects of R_{sh} R_s are neglected (R_s and R_{sh} are supposed to be null and infinite respectively)[4],[7],[3].

The simplified bond graph model is given by Figure7.

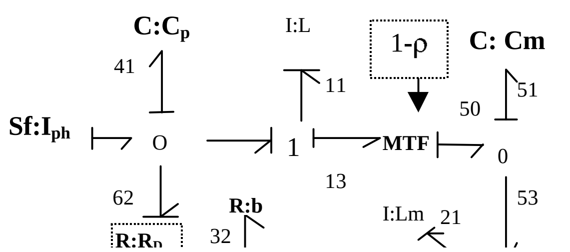

3 Equation formulation

To further understand the dynamic behaviour of our PV system, we derive the nonlinear state equation from bond graph model (Fig.7).

At a first stage we study this dynamic behaviour in open loop. The control of the system is made through the duty cycle ρ of the converter. The developed equation set are used for stability analysis using linear techniques.

3.1 Nonlinear state equation

The bond graph model preserves the same causality for the remained elements (fig.7). Once this simplification is done, the state equation can be easily obtained. The state vector x is composed of the energy variables in integral causality (p on I elements and q on C elements), that is

$$x = \begin{bmatrix} p_{11} & p_{21} & p_{31} & q_{41} & q_{51} \end{bmatrix}^t = \begin{bmatrix} p_L & p_{Lm} & p_J & q_{cp} & q_{cm} \end{bmatrix}^t \tag{7}$$

The state equation is:

$$\dot p_L = \frac{1}{C_p} q_{cp} - \frac{1-\rho}{C_m} q_{cm}$$

$$\dot p_{Lm} = -\frac{R_m}{L_m} p_{Lm} - \frac{K_b}{J} p_J + \frac{1}{C_m} q_{cm}$$

$$\dot p_J = \frac{K_b}{L_m} p_{Lm} - \frac{K_T + b}{J} p_J$$

$$\dot q_{cp} = -\frac{1}{L} p_L - \psi^{-1} R_D\left(\frac{q_{cp}}{C_p}\right) \frac{q_{cp}}{C_p} + I_{ph}$$

$$\dot q_{cm} = \frac{1-\rho}{L} p_L - \frac{1}{L_m} p_{Lm}$$

(8)

3.2 Linearisation of state equation

The equation set (8) is nonlinear. For analysis purposes, it is useful to linearise these equations around a given steady-state condition.(peak power point in our case). There are two stages to this process: finding the steady-state and after that perform the linearisation, [4],[7].

3.2.1 Finding the steady state

For PV systems, the operating point is currently chosen near the peak power point voltage V_{po}. To find this steady-state with V_{po} voltage, we must at first solve (4) and later the equation set (9) corresponding to $\dot x = 0$, and $x = \bar x$,

$$0 = \frac{1}{C_p} \bar q_{cp} - \frac{1-\bar\rho}{C_m} \bar q_{cm}$$

$$0 = -\frac{R_m}{L_m} \bar p_{Lm} - \frac{K_b}{J} \bar p_J + \frac{1}{C_m} \bar q_{cm}$$

$$0 = \frac{K_b}{L_m} \bar p_{Lm} - \frac{K_T + b}{J} \bar p_J$$

$$0 = -\frac{1}{L} \bar p_L - \psi^{-1} R_D\left(\frac{\bar q_{cp}}{C_p}\right) \frac{\bar q_{cp}}{C_p} + I_{ph}$$

$$0 = \frac{1-\bar\rho}{L_m} \bar p_L - \frac{1}{L_m} \bar p_{Lm}$$

(9)

$\bar p_L$, $\bar p_{Lm}$, $\bar p_J$, $\bar q_{cp}$ and $\bar q_{cm}$ represent the state variables at steady-state. Output variables can then be deduced at steady state:

$$\bar I_L = \frac{\bar p_L}{L}, \quad \bar I_{Lm} = \frac{\bar p_{Lm}}{L_m}, \quad \bar V_m = \frac{\bar q_{cm}}{C_m}, \quad \bar\Omega = \frac{\bar p_J}{J}. \tag{10}$$

3.2.2 Linearisation of bond graph model

The linearisation can be applied by following two different ways, which lead to the same linearised state model:

- directly on the non linear state equation,
- from the bond graph model.

Since we used the bon graph technique we propose to follow the second way.

To obtain the linearised bond graph model, we apply the technique introduced in Karnopp[8].

At a first stage we begin by linearising the non linear element R_D. With affected input effort causality, the linearised R_D bond graph model is as follows:

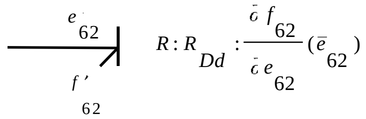

Fig.8. linearised bond graph model of R_D

R_{Dd} is the PV array diode dynamic resistance.

At a second stage we linearise the modulated transformer MTF of the boost converter. With affected input flow causality the linearised MTF bond graph model is as follows:

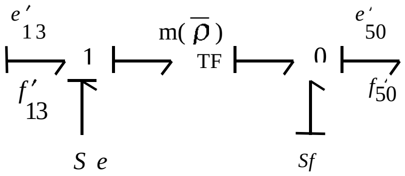

Fig. 9. Linearised MTF bond graph model

with $m(\bar{\rho}) = 1 - \bar{\rho}$, Sf and Se are exposed as:

$$Se = -\frac{dm}{d\rho}(\bar{\rho})\bar{e}_{50}\,\rho' = \bar{e}_{50}\,\rho' = \bar{V}_m\,\rho' \qquad (11)$$

$$Sf = \frac{dm}{d\rho}(\bar{\rho})\bar{f}_{13}\,\rho' = -\bar{f}_{13}\,\rho' = -\bar{I}_L\,\rho \qquad (12)$$

To establish the global linearised bond graph PV system we take into account just the dynamic parts and so constant source $Sf = I_{ph}$ is eliminated.

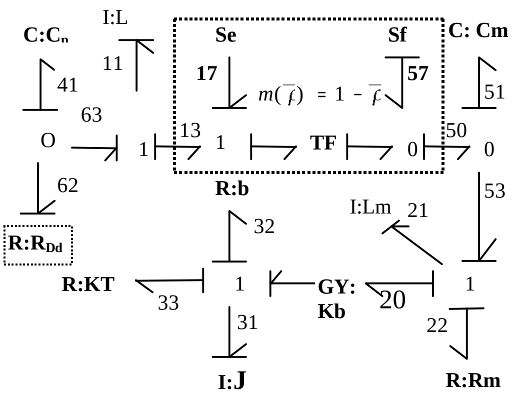

Fig. 10. linearised bond graph model of the PV system

The vector composed by dynamic sources is $\begin{bmatrix} e'_{17} \\ f'_{57} \end{bmatrix} = \begin{bmatrix} Se{:}\bar{V}_m\,\rho' \\ Sf{:}-\bar{I}_L\,\rho \end{bmatrix}$, with $u' = \rho'$ the dynamic control variable.

The linear state equation $\dot{x}' = Ax' + Bu'$ is then easily deduced from the linearised bond graph model shown in Figure 10.

$$\begin{bmatrix} \dot{p}'_L \\ \dot{p}'_{Lm} \\ \dot{p}'_J \\ \dot{q}'_{cp} \\ \dot{q}'_{cm} \end{bmatrix} = \begin{bmatrix} 0 & 0 & 0 & \frac{1}{C_p} & -\frac{1-\bar{\rho}}{C_m} \\ 0 & -\frac{R_m}{L_m} & -\frac{K_b}{J} & 0 & \frac{1}{C_m} \\ 0 & \frac{K_b}{L_m} & -\frac{K_T + b}{J} & 0 & 0 \\ -\frac{1}{L} & 0 & 0 & -\frac{1}{R_{Dd}\,C_p} & 0 \\ \frac{1-\bar{\rho}}{L} & -\frac{1}{L_m} & 0 & 0 & 0 \end{bmatrix} \begin{bmatrix} p'_L \\ p'_{Lm} \\ p'_J \\ q'_{cp} \\ q'_{cm} \end{bmatrix} + \begin{bmatrix} \bar{V}_m \\ 0 \\ 0 \\ 0 \\ -\bar{I}_L \end{bmatrix} \rho'$$

(13)

Equation (13) is identical to the result obtained by the linearisation of the nonlinear equations [11][3].

$p'_L, p'_{Lm}, p'_J, q'_{cp}, q'_{cm}, I'_L, I'_{Lm}, \Omega', V'_p, V'_m, \rho'$ characterise the variation of $p_L, p_{Lm}, p_J, q_{cp}, q_{cm}$ $I_L, I_{Lm}, \Omega, V_p, V_m, \rho$ around the nominal operating point $\bar{p}_L, \bar{p}_{Lm}, \bar{p}_J, \bar{q}_{cp}, \bar{q}_{cm}, \bar{I}_L, \bar{I}_{Lm}, \bar{\Omega}, \bar{V}_p, \bar{V}_m, \bar{\rho}$.

4 Study of stability

4. 1 Study of transfer function poles

The stability of this PV system is checked by computing the roots of the characteristic equation. Routh-Hurwitz criterion was used and none roots of the characteristic equation lie in the right half of the s-plan poles.

$$P(\lambda) = \det(\lambda I - A) = \lambda^4 + a_3\lambda^3 + a_2\lambda^2 + a_1\lambda + a_0 = 0$$

(14)

$a_4, a_3, a_4, a_2, a_1, a_0$ are function of experimental assembly parameters cited above and especially of R_{Dd}

For this PV system R_{Dd} is positive and so the system is always stable. In fact the linearity of the characteristic shaft torque-velocity ($\Gamma = K_T\,\Omega$) makes the system analogous to an autonomous load [4].

Figure 11 shows the variation of dominant poles of transfer function with PV array voltage (V_p). No positive real poles then the system is stable for all PV array voltage area .

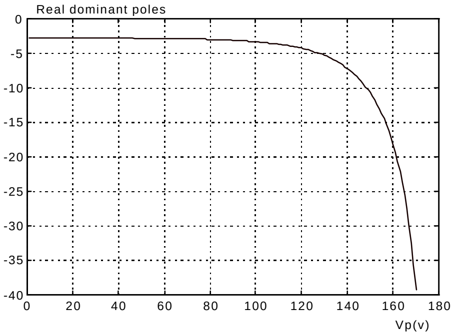

Fig.11 Real dominant poles functionV_p

4.2 Study of transfer function zeros

For monocontrolled system, the zeros are the roots of transfer function numerator. In this study we are interested to the angular velocity transfer function which is the most significant for us. This latter is given by:

$$\frac{\Omega'(s)}{\rho'(s)} = (b_2 s^2 + b_1 s + b_0)\varphi^{-1}(s) \tag{15}$$

with $\varphi(s) = \det(s.I - A)$,

$$b_2 = -\frac{\bar{I}_L K_b}{J^2 . L_m}, \tag{16}$$

$$b_1 = \frac{\bar{V}_m (1-\bar{\rho}) K_b}{C_m J^2 . L_m} - \frac{K_b \bar{I}_L}{J^2 L_m R_{Dd} C_p}, \tag{17}$$

$$b_0 = \frac{K_b \bar{V}_m (1-\bar{\rho})}{R_{Dd} C_p C_m J^2 L_m} - \frac{\bar{I}_L K_b}{J^2 L L_m C_p}, \tag{18}$$

These values can be directly deduced from the bond graph model (Fig.10) by using Mason's rule [5].

The study of these zeros of the transfer function showed a non minimal phase response, caused by a positive real roots in the numerator, for operating limited area PV array voltage. This latter depend on experimental assembly parameters. To confirm this idea we give computing results using different values of the storage capacitor C_p (Fig.12, 13). However a same study has been done for a PV system with buck converter configuration showing non minimal phase response corresponding to the all operating voltage in which $V_p<V_{po}$, [3].

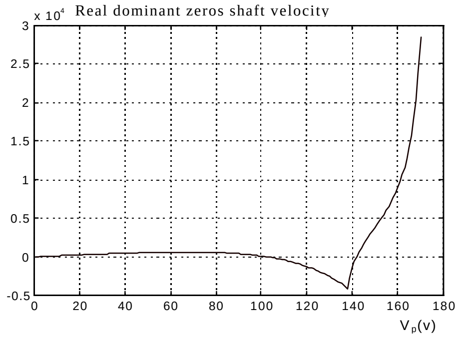

Fig.12. Real dominant zeros shaft velocity function V_p With $C_p=10^{-5}$ F.

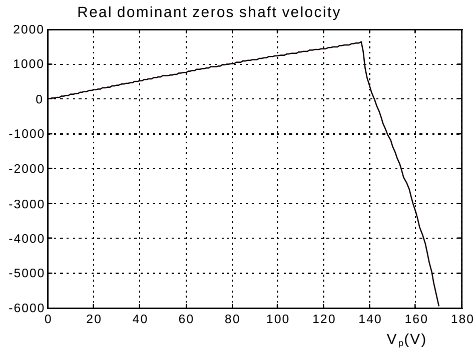

Fig.13. Real dominant zeros shaft velocity function V_p With $C_p=10^{-4}$ F

5. Simulation results

To further understand the dynamics of this experimental PV plant, computer simulations of transient responses in several situations were carried out by using 20-sim packages.

Figure 14 is showing a transient output variables in the starting-up in direct matching (without DC-DC converter). In this figure we represent all the output variables (I_{Lm}, Ω, V_p). At steady state the corresponding values are $\bar{I}_{Lm} = 5.75A$, $\bar{\Omega} = 115 rd/s$ and $\bar{V}_p = 162V$. These values are far from the peak power point corresponding to a PV array voltage $\bar{V}p = 130V$. These results confirm the necessity of the MPPT converters in that situation.

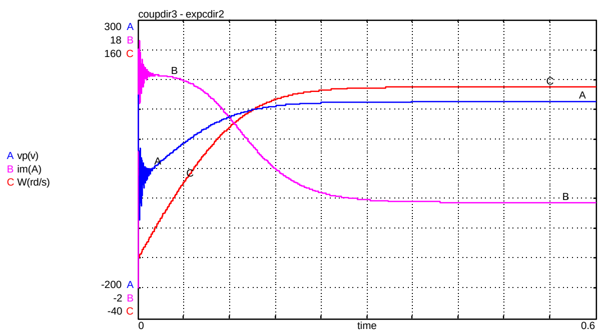

Fig.14. transient output variables in the starting-up in direct matching (without DC-DC converter) .

Figure 15 shows the transient output variables in the starting-up by using the MPPT boost converter. In this figure we represent all the output variables. At steady state the corresponding values are:

$\bar{I}_L = 12.2\,A, , \bar{I}_{Lm} = 7.5\,A, \bar{\Omega} = 150\,rd/s, \bar{V}_p = 130\,v$,

and $\bar{V}_m = 212\,v$.

From these values we deduce that the electromechanical load is receiving the maximum power from the PV generator via the MPPT boost converter.

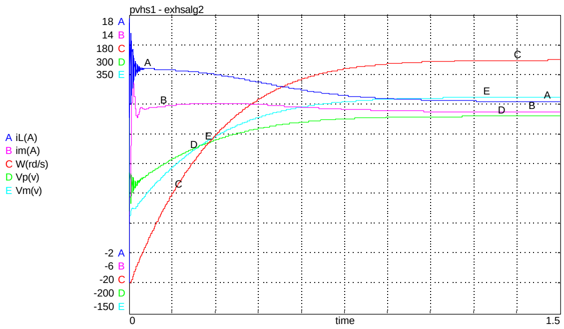

Fig.15. transient output variables in the starting-up With MPPT boost converter

Figure 16 (shows the transient response of shaft velocity Ω and PV array voltage V_p in the operating starting-up and with step disturbance on ρ . For this simulation and above ones we use directly the non linear bond graph model (Fig.7).

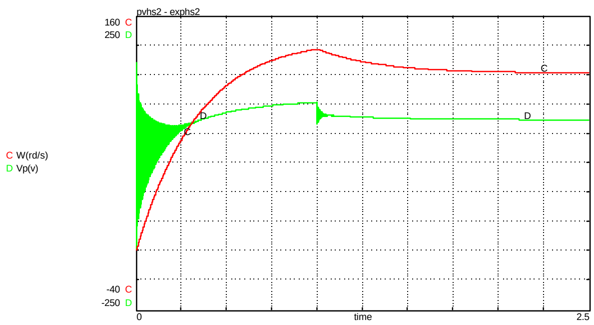

Figure. 16. Transient response of Ω and V_p in the operating starting-up and with step disturbance on ρ

To confirm the computing results shown above, we give finest simulation of the transient response of velocity (Ω') in response to a step disturbance in the switch duty-cycle ρ at V_p=V_{po} using different values of the storage capacitor C_p with boost converter (Fig.17). For these simulations we used the linearised bond graph model with small perturbation on ρ. The results are interesting from a structural, a computational, and a control point of view.

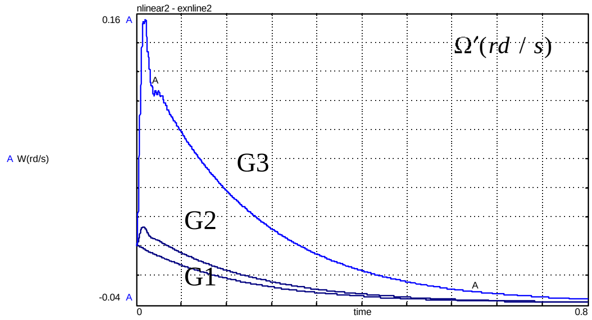

Fig.17. Transient response of shaft velocity G1:C_p=10^{-5} F, G2:C_p=10^{-4} F, G3:C_p=10^{-3} F at V_p=V_{po} (ρ' = 0.02) with boost converter

To compare dynamic performances of buck and boost configurations in such applications, we give simulation of the transient response of velocity (Ω') in response to a step disturbance in the switch duty-cycle ρ at Vp>Vpo, Vp=Vpo and Vp<Vpo with buck converter (Fig.18). For the PV system with buck configuration, a deep study in [3] has shown that positive real zeros are obtained for operating PV array voltage inferior to V_{po} These results confirm the opinions which stated that a buck converter does not assure minimal phase responses whatever the parameter values of this PV system may be [7].

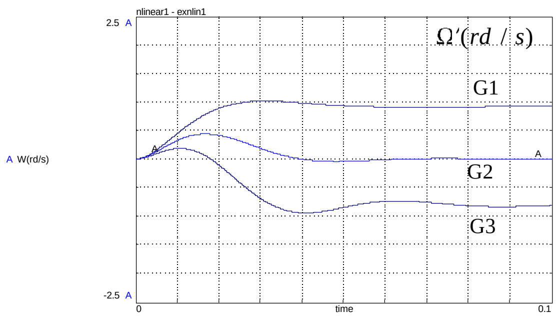

Fig.18. Transient response of shaft velocity G1: Vp>Vpo, G2: Vp=Vpo, G3 Vp<Vpo (ρ' = 0.01) with buck converter

From the results given above we deduce that PV systems, with boost configuration, are always stable. However, a Non Minimal Phase Responses (NMPR), due to positive real roots in the numerator of the velocity transfer function are detected. These NMPR lead to mechanical problems hardly bearable by electromechanical

machines. In fact these NMPR are harmful leading to shaft torque perturbations and then causing mechanical vibrations and hence the load destruction. Furthermore, in dynamical regime these NMPR prevent the optimal transfer of the electric power from PV sources to loads.
The positive real zeros computed above depend on experimental assembly parameters. Therefore a good sizing of the latters will reliably avoid mechanical problems.

6 Conclusion

A bond graph model of a PV system was developed. Discussion of problems causality leads to the use of a simplified model giving more facilities to study the dynamic behaviour and the control of such systems.

Transient responses have been computed and non minimal phase responses were detected. These responses were confirmed by a deep study in which we establish the linearised state equation and the associated transfer function of this PV plant.

At a first stage we have studied the system in open loop. The study in closed loop will be handled in a second stage in which we try to develop a control system that will track the maximum power point of the PV array. In this study we project the use of robust control strategies.

References

[1] Alghuwainem.S.M,″Matching of a DC motor to a photovoltaic generator using a step converter with a current looked loop″. IEEE transactions on Energy Conversion, vol 9 , n°1, 1994,pp. 192-198
[2] Allard.B, Morel.H, Lautier.Ph, and Retif.J.M. 1997. ″Bond graphs for averaged modelling of power electronic converters ″ Proceeding of ICBGM'97, vol 29, pp 201-206.
[3] Andoulsi.R, Mami.A, Dauphin-Tanguy.G, and Annabi.M, ″Bond graph modelling of a photovoltaic generator coupled to a DC motor ″.WMC'99, ICBGM'99 San Francisco, January 1999, pp 371-378.
[4] Ben Naceur.H, Dhifaoui.R, Annabi.M. 1994. ″Compensation par retour d'état de la dynamique d'un système générateur photovoltaï que, convertisseur et moteur à courant continu.″ CMGE'94 - Tunis, EP 50-57.
[5] Brown F.T. 1972. ″Direct application of the loop rule to bond graphs.″ Journal of Dynamic System., 253-261.
[6] Dauphin-Tanguy.G, and Rombaut.C ″ why a unique causality in the elementary commutation cell bond graph model of a power electronic converter″. In proceedings of the international conference on systems, Man and cybernetics. IEEE. le Touquet vol.1, pp.257-263, 1993.
[7] Hamdi.L. 1991. ″Onduleur autonome triphasé compact asservi pour des générateurs de puissance finie.″ Thèse 91 (AIX-MARSEILLE III)., France.
[8] Karnopp.D. 1977. ″ Power and Energy in Linearized Physical Systems ″, Journal of FranKline Institute, vol 303, n°1, 86-98.
[9] Madansure.V.N, Banerjee.S, Mukherjee.A, Chattopadhyay.P.K. ″Modelling and simulation of PV-powered intermittent load systems by bond graph technique.″ Solar Energy, vol.55, n°5, 1997. pp 367-375.
[10] Madansure.V.N, Banerjee.S, Mukherjee.A, Chattopadhyay.P.K. ″Bond graph Modelling and simulation of spice-pounding machines fed from a photovoltaic source.″ International Journal of Energy Research, vol 21,1997 ,pp 683-694.
[11] Rimaux.S. 1995, ″Etude des propriétés structurelles de certaines classes de systèmes physiques non lineaires modelisés par bond graph″. Thèse1995, USTLille,France.
[12] Singer.S, Appelbaum.J, ″Starting characteristcs of current motors powred by solar cells″ , IEEE Transactions on Energy conversion, vol.8n°1,1993,pp.47-53.
[13] Suehrcke.H, Appelbaum.J and Reshef.B ″Modelling a permanent magnet DC motor/centrifugal pump assembly in a photovoltaic energy system″. Solar Energy vol 59,n°1-3,1997, pp.37-42.